

On the Late-Time Behavior of Tracer Test

Breakthrough Curves

Roy Haggerty

Dept. of Geosciences

Oregon State University

Corvallis, OR 97331-5506

RECEIVED
JUN 20 2000
OSTI

Sean A. McKenna and Lucy C. Meigs

Sandia National Laboratories

Geohydrology Dept.

P.O. Box 5800, MS-0735

Albuquerque, NM 87185-0735

Submitted to Water Resources Research

Sandia Technical, QA, Management Review Completed 12/8/99

1 Abstract

2 We investigated the late-time (asymptotic) behavior of tracer test breakthrough
3 curves (BTCs) with rate-limited mass transfer (e.g., in dual or multi-porosity systems)
4 and found that the late-time concentration, c , is given by the simple expression:

5
$$c = t_{ad} \left(c_0 g - m_0 \frac{\partial g}{\partial t} \right), \quad \text{for } t \gg t_{ad} \text{ and } t_\alpha \gg t_{ad}$$

6 where t_{ad} is the advection time, c_0 is the initial concentration in the medium, m_0 is the 0th
7 moment of the injection pulse; and t_α is the mean residence time in the immobile domain
8 (i.e., the characteristic mass transfer time). The function g is proportional to the residence
9 time distribution in the immobile domain; we tabulate g for many geometries, including
10 several distributed (multirate) models of mass transfer. Using this expression we examine
11 the behavior of late-time concentration for a number of mass transfer models. One key
12 result is that if rate-limited mass transfer causes the BTC to behave as a power-law at
13 late-time (i.e., $c \sim t^{-k}$), then the underlying density function of rate coefficients must also
14 be a power-law with the form α^{k-3} as $\alpha \rightarrow 0$. This is true for both density functions of
15 first-order and diffusion rate coefficients. BTCs with $k < 3$ persisting to the end of the
16 experiment indicate a mean residence time longer than the experiment and possibly
17 infinite, and also suggest an effective rate coefficient that is either undefined or changes
18 as a function of observation time. We apply our analysis to breakthrough curves from
19 Single-Well Injection-Withdrawal tests at the Waste Isolation Pilot Plant, New Mexico.

DISCLAIMER

This report was prepared as an account of work sponsored by an agency of the United States Government. Neither the United States Government nor any agency thereof, nor any of their employees, make any warranty, express or implied, or assumes any legal liability or responsibility for the accuracy, completeness, or usefulness of any information, apparatus, product, or process disclosed, or represents that its use would not infringe privately owned rights. Reference herein to any specific commercial product, process, or service by trade name, trademark, manufacturer, or otherwise does not necessarily constitute or imply its endorsement, recommendation, or favoring by the United States Government or any agency thereof. The views and opinions of authors expressed herein do not necessarily state or reflect those of the United States Government or any agency thereof.

DISCLAIMER

**Portions of this document may be illegible
in electronic image products. Images are
produced from the best available original
document.**

1. Introduction

2 Mass transfer continues to be cited as a critical transport process in groundwater,
3 soils, and streams. Estimation of rate coefficients (for both diffusion and sorption) is
4 highly sensitive to the late-time behavior of breakthrough curves (BTCs). Indeed, recent
5 studies have shown that the late-time data (i.e., after the advective peak has passed) may
6 be the most important data for estimation of both the capacity coefficient and the rate
7 coefficient or density function of rate coefficients [e.g., *Farrell and Reinhard*, 1994;
8 *Wagner and Harvey*, 1997; *Werth et al.*, 1997; *Haggerty and Gorelick*, 1998; *Haggerty et*
9 *al.*, in review]. With improvements in experimental and analytical techniques,
10 concentration observations are now frequently available from laboratory and field
11 experiments over several orders of magnitude of both time and concentration. Therefore,
12 the examination of late-time behavior of BTCs is both feasible and critically important to
13 the evaluation of rate-limited mass transfer, particularly if discrimination between
14 different models of mass transfer is desired.

15 A rapidly growing body of recent work on mass transfer and transport has
16 extended the basic model of single-rate mass transfer [e.g., *Coats and Smith*, 1964; *van*
17 *Genuchten and Wierenga*, 1976; *Cameron and Klute*, 1977; *Rao et al.*, 1980] or two-rate
18 mass transfer [e.g., *Brusseau et al.*, 1989] to models with distributed, or multiple rates of
19 mass-transfer described by a density function of rate coefficients and primarily applied to
20 laboratory data [*Connaughton et al.*, 1993; *Lafolie and Hayot*, 1993; *Pedit and Miller*,
21 1994, 1995; *Backes et al.*, 1995; *Chen and Wagenet*, 1995; *Haggerty and Gorelick*, 1995;
22 *Ahn et al.*, 1996; *Chen and Wagenet*, 1997; *Culver et al.*, 1997; *Cunningham et al.*, 1997;

1 *Sahoo and Smith, 1997; Werth et al., 1997; Cunningham and Roberts, 1998; Deitsch et*
2 *al., 1998; Haggerty and Gorelick, 1998; Kauffman et al., 1998; Lorden et al., 1998;*
3 *McLaren et al., 1998; Hollenbeck et al., 1999; Stager and Perram, 1999]. It should be*
4 *noted, however, that the concept of multiple time-scales of mass transfer has been*
5 *employed for at least three orders of magnitude, primarily in chemical engineering and*
6 *soil physics [Ruthven and Loughlin, 1971; Villermaux, 1981; Rao et al., 1982; Neretnieks*
7 *and Rasmussen, 1984; Rasmussen, 1985; Fong and Mulkey, 1990; Valocchi, 1990], as*
8 *have multiple time-scales of reaction in chemistry [e.g., Albery et al., 1985 and many*
9 *others].*

10 The work of *Haggerty and Gorelick [1995, 1998]* is particularly important to this
11 current work. These papers develop and apply the “multirate” model, which is a
12 transport model with a spatially-uniform density function of first-order mass transfer rate
13 coefficients. These papers show that any density function of diffusion rate coefficients
14 may be represented in a transport model by a different, but exactly equivalent, density
15 function of first-order rate coefficients.

16 The multirate model has been applied to field data collected in a set of single-well
17 and two-well convergent flow tracer tests conducted in a fractured dolomite (*Haggerty et*
18 *al., in review*). After pulse injections of solute, the BTC data in the Single-Well
19 Injection-Withdrawal (SWIW) tests showed a power-law behavior at late-time
20 (i.e., $c \sim t^k$). Within the SWIW tests, k ranged from 2.1 to 2.8. The diffusion rate
21 coefficients in this application were described by an assumed lognormal density function
22 of diffusion rate coefficients, and interpretation of the BTC data focused on defining the
23 mean and standard deviation of this lognormal density function to match data observed in

1 the tail of the BTC. While the lognormal density function provided excellent matches to
2 the data, the details of the power-law behavior of the tail of the BTC were left for a
3 future investigation. In particular, two issues were left: (1) an understanding of the
4 density functions of rate coefficients that could lead to late-time power-law behavior; and
5 (2) the range of late-time slopes that can be provided by a lognormal density function.

6 A power-law plots as a straight line on a double-logarithmic graph.
7 Consequently, in this paper we will frequently refer to the value of the power k as the
8 "slope". Although the slope is always negative, for the sake of brevity, we will refer only
9 to its absolute value.

10 Power-law behavior at late time in BTCs has been noted in a number of other
11 laboratory and field experiments. *Farrell and Reinhard* [1994] and *Werth et al.* [1997]
12 observed power-law BTC and mass recovery curves with sorbing organic solutes in
13 unsaturated media. *Cunningham et al.* [1997] were able to represent the *Werth et al.*
14 [1997] data with a gamma density function of diffusion rate coefficients, while *Haggerty*
15 and *Gorelick* [1998] were able to approximate the power-law behavior with a lognormal
16 density function of diffusion rate coefficients. Both *Cunningham et al.* [1997] and
17 *Haggerty and Gorelick* [1998] noted the inability of conventional models of mass
18 transfer to yield the appropriate power-law behavior. Power-law behavior with a slope
19 of 3/2 has been observed in field data from the Grimsel test site and has been adequately
20 explained with conventional (single-rate) matrix diffusion [*Eikenberg et al.*, 1994;
21 *Hadermann and Heer*, 1996]. However, single-rate diffusion is only able to yield a
22 power-law of exactly $t^{3/2}$, and can only maintain this behavior slightly longer than the

1 mean immobile-domain residence time ($t_a = \alpha^2/15D_a$ for spheres and $\alpha^2/3D_a$ for layers),
2 where D_a is the apparent diffusivity and α is the half-thickness of the immobile domain.
3 Power-law behavior such as that observed in *Farrell and Reinhard* [1994]; *Werth et al.*
4 [1997]; or *Meigs and Beauheim* [in review] cannot be explained with conventional
5 single-rate diffusion. *Jaekel et al.* [1996] showed that power-law BTCs result from a
6 pulse injection of solute and equilibrium Freundlich sorption. Unfortunately, none of the
7 data sets mentioned above are explained by this (the *Meigs and Beauheim* tracers were
8 non-sorbing, and equilibrium Freundlich sorption is insufficient to explain the power-
9 laws in the other data sets [*Werth et al.*, 1997]).

10 The late-time (asymptotic) behavior of BTCs undergoing first-order linear
11 nonequilibrium sorption has been examined by *Vereecken et al.* [1999]. *Vereecken et al.*
12 [1999] develop late-time expressions for the BTC that are valid for time-varying
13 velocity, but only after a pulse injection and in media with one- or two-site
14 nonequilibrium sorption.

15 The purpose of this paper is to explore the nature of tailing in mobile-immobile
16 (dual porosity) tracer test BTCs for a wide variety of linear mass transfer models.
17 Specifically, we have the following objectives: (1) develop an analytic expression for the
18 late-time BTCs for transport experiencing a distribution of either first-order sorption or
19 diffusion time-scales and for both pulse injections and media with non-zero initial
20 concentrations; (2) examine the information that can be provided by the late-time
21 behavior of the BTC; (3) examine BTCs that exhibit power-law behavior at late time and
22 the implications for mass transfer. Particular expressions describing the late-time BTCs

1 for single-rate models with both infinite and finite immobile domains, as well as
2 multirate models with first-order and diffusion rate coefficients defined by lognormal,
3 gamma and power-law density functions are provided. Implications of the late-time
4 slopes defined by these equations are discussed with respect to mass transfer processes,
5 including implications for estimates of the mean residence time in the immobile zone (or,
6 equivalently, a characteristic mass transfer time). The power-law late-time behavior of
7 BTCs in two SWIW tests from the WIPP site are examined.

8 **2. Mathematical Development**

9 **2.1. General case**

10 **2.1.1. Late-Time Solution for Concentration:**

11 The mass balance equation for a solute advecting and dispersing in 1-D (i.e.,
12 along a single stream tube), and interacting with rock via diffusion, linear equilibrium
13 sorption, and/or linear nonequilibrium sorption is:

14
$$\frac{\partial}{\partial x} \left(\frac{\alpha_L v}{R_a} \frac{\partial c}{\partial x} - \frac{v}{R_a} c \right) = \frac{\partial c}{\partial t} + \Gamma(x, t) \quad (1)$$

15 where α_L [L] is longitudinal dispersivity; v [LT⁻¹] is pore-fluid velocity; R_a [-] is the
16 retardation factor in the mobile (advective, effective or kinematic) porosity; c [ML⁻³] is
17 solute concentration within the advective porosity; and $\Gamma(x, t)$ [ML⁻³T⁻¹] is the source-
18 sink term for mass exchange with the immobile (matrix or diffusive) porosity and
19 nonequilibrium sorption sites. From this point forward, we will adopt the terminology of

1 "mobile" and "immobile" domains and concentrations, which refer to either sorption or
 2 diffusion. We will employ the uniform initial conditions

3 $c(x, t=0) = c_{im}(x, z, t=0) = c_0$ (2a)

4 where c_{im} [ML⁻³] is solute concentration within the immobile domain, which may, in the
 5 case of diffusion, be a function of a second spatial coordinate z oriented normal to the
 6 mobile-immobile domain interface. We will also employ the boundary conditions

7 $c(x=0, t) = m_0\delta(t)$ (2b)

8 $c(x \rightarrow \infty, t) = c_0$ (2c)

9 where m_0 [MTL⁻³] is the zeroth moment of the BTC; c_0 [ML⁻³] is the initial concentration
 10 in the system; and $\delta(t)$ [T⁻¹] is the Dirac delta. The Dirac injection is never met in
 11 practice. However, as long as the duration of the pulse is much shorter than the mean
 12 residence time in the immobile zone, (2b) will be a sufficiently good approximation. For
 13 a finite pulse injection with constant velocity, the zeroth moment m_0 is the injected
 14 concentration multiplied by injection time.

15 For initial and boundary conditions (2a-c), then at late time:

16 $\alpha_L \frac{\partial c}{\partial x} \ll c, \quad \text{for } t \gg t_{ad}$ (3)

17 where t_{ad} [T] is the average advective residence time (equal to LR_d/v if velocity is
 18 constant in space). In other words, once the input pulse has advected far past the point of

1 observation L , then dispersion has a negligible effect on concentration. Similarly, if the
 2 immobile domain has a long mean residence time relative to advection, then at late time:

3 $\frac{\partial c}{\partial t} \ll \Gamma(x, t), \text{ for } t \gg t_{ad} \text{ and } t_a \gg t_{ad}$ (4)

4 where t_a [T] is the mean residence time in the immobile domain. In other words,
 5 concentration change at late time is dominated by exchange between the mobile and
 6 immobile domains if the average immobile domain residence time is longer than the
 7 advective time. Note that from this point forward, it will be assumed that $t_a \gg t_{ad}$ and
 8 $t \gg t_{ad}$ unless otherwise stated. Therefore, the equation (1) may be re-written:

9 $-\frac{\partial}{\partial x} \left(\frac{v}{R_a} c \right) = \Gamma(x, t)$ (5)

10 By integration we can obtain a solution for concentration at late time:

11 $c(x=L, t) = - \int_0^L \frac{R_a(x)}{v(x)} \Gamma(x, t) dx$ (6)

12 where L [L] is the distance from point of injection to point of observation along the flow
 13 path. If velocity, retardation, and the parameters and functions that comprise $\Gamma(x, t)$ are
 14 spatially uniform, then this leaves us with a very simple expression for concentration at
 15 late time:

16 $c(x=L, t) = -t_{ad} \Gamma(t)$ (7)

1 The spatially-variable case is left for a future paper. From this point on the dependency
 2 of c on $x=L$ and t is implicitly assumed.

3 **2.1.2. Source-Sink Term $\Gamma(t)$:**

4 The source-sink term $\Gamma(t)$ is the rate of loss or gain of concentration to or from
 5 the immobile domain (loss at early time and gain at late time). For any linear mass
 6 transfer problem with uniform initial conditions it is possible to express the source-sink
 7 term as the following, which is valid at all times:

8
$$\Gamma(t) = \int_0^t \frac{\partial c(t-\tau)}{\partial \tau} g(\tau) d\tau = \frac{\partial c}{\partial t} * g = c^* \frac{\partial g}{\partial t} + c g_0 - c_0 g \quad (8)$$

9 where $g(t)$ is a "memory function" to be defined; $*$ represents the convolution product; g_0
 10 is the memory function at $t = 0$; and c_0 [ML⁻³] is the initial concentration. Note that the
 11 Laplace transform of (8) is commonly used in analytical solutions [e.g., *Villermaux*, 1974
 12 and many others since], and that the last transformation in (8) is most easily derived in
 13 the Laplace domain. Equation (8) has been expressed explicitly in the time domain by
 14 e.g., *Peszynska* [1996] and *Carrera et al.* [1998], and results in an integro-partial
 15 differential equation when substituted back into (1). The memory function $g(t)$ may be
 16 physically interpreted as the capacity coefficient (β_{tot} , see Section 2.3) multiplied by the
 17 residence time distribution in the immobile domain, given a Dirac pulse at the surface.
 18 The derivative of $g(t)$ is proportional to what is commonly called in statistical physics the
 19 probability of first return or distribution of first passage times [e.g., *Bouchaud and*
 20 *Georges*, 1990, p. 271-272].

1 We desire to find a closed-form expression for the source-sink term in (8),
 2 accurate at late time, that may be substituted into (7). We recognize the following
 3 characteristics of $\Gamma(t)$: (1) at early time the function represents rapid loss from a high-
 4 concentration pulse in the mobile domain to the immobile domain; and (2) at late time
 5 the function represents slow gain to the mobile domain (which has very low
 6 concentration) from the immobile domain. To obtain a solution that is accurate at late
 7 time, we therefore require an approximate function for mobile-domain concentration that
 8 has the correct pulse size at early time, and that is approximately zero at late time. Such
 9 an approximation is available in $c \equiv m_0 \delta(t)$, where m_0 is the zeroth moment of the
 10 injection. Note that this approximation is used only for calculating the source-sink term,
 11 and not as an approximation for late-time concentration itself. That this approximation is
 12 sufficient will become apparent when the results are compared to a full numerical
 13 solution. Employing the properties of convolution, (8) can now be expressed:

$$14 \quad \Gamma(t) \equiv m_0 \frac{\partial g}{\partial t} - c_0 g, \quad \text{for } t \gg t_{ad} \text{ and } t_a \gg t_{ad} \quad (9)$$

15 The general form of the memory function is [modified from Carrera et al., 1998]

$$16 \quad g(t) = \int_0^\infty \alpha b(\alpha) e^{-\alpha t} d\alpha \quad (10)$$

17 where α is a rate coefficient and $b(\alpha)$ is a density function of first-order rate coefficients.
 18 Note two differences between our definition of the memory function and that of Carrera
 19 et al. [1998, Eqn. (15), p. 182]. First, our memory function $g(t)$ includes the constants
 20 that are placed before the source-sink term in Carrera et al.'s mass balance equation.

1 Secondly, although Carrera et al. [1998] express (10) as a discrete function, the more
 2 general expression is as a continuous function, allowing for density functions of diffusion
 3 rate coefficients, etc. Various density functions $b(\alpha)$ are given in Table 1, along with the
 4 corresponding memory function $g(t)$.

5 We note that (10) is the Laplace transform of $\alpha b(\alpha)$, where t substitutes for the
 6 Laplace variable. We also use the property of the Laplace transform [e.g., Roberts and
 7 Kaufman, 1966, p. 4]

$$8 \quad \text{Lap}\{\alpha^2 b(\alpha)\} = -\frac{\partial g}{\partial t} \quad (11)$$

9 where $\text{Lap}\{*\}$ indicates the Laplace transform.

10 Employing (7), (9), (10), and (11), we can now write an approximation for
 11 concentration at late time:

$$12 \quad \begin{aligned} c &= t_{ad} \left(c_0 g - m_0 \frac{\partial g}{\partial t} \right) \\ &= t_{ad} \int_0^{\infty} (c_0 + \alpha m_0) \alpha b(\alpha) e^{-\alpha t} d\alpha \\ &= t_{ad} \text{Lap}\{(c_0 + \alpha m_0) \alpha b(\alpha)\} \end{aligned} \quad (12)$$

13 All forms of (12) are equivalent and are useful in different ways for understanding the
 14 late-time behavior of BTCs. We expect that in most applications only one of c_0 or m_0
 15 will be non-zero; however, (12) holds true regardless of the values of c_0 and m_0 . Note
 16 that the late-time concentration can be calculated for various density functions $b(\alpha)$ using
 17 $g(t)$ supplied in Table 1.

1 At this point, we re-emphasize the restrictions on Equation (12). These are (1)
2 time is much greater than the advection time; (2) the mean residence time in the
3 immobile domain is much greater than the advection time; and (3) time is much greater
4 than the duration of the injection pulse, meaning that an impulse (Dirac) function is a
5 valid approximation to the injection. In a heterogeneous velocity field, restrictions (1)
6 and (2) mean that both time and mean residence time in the immobile domain must be
7 much greater than the sum of advection time across a control plane and the standard
8 deviation of that advection time. In particular, a power-law distribution of advection
9 times (such as invoked by e.g., *Berkowitz and Scher* [1997]) would invalidate the use of
10 (12).

11 2.2. Notes on Application of Equation (12)

12 Equation (12) presents an interesting theoretical development for two reasons.
13 First, the late-time behavior of the BTC is easily obtained for a wide variety of density
14 functions $b(\alpha)$ using any comprehensive table of Laplace transforms. Equation (12) is
15 simpler for first-order mass transfer than the equations developed by *Vereecken et al.*
16 [1999]. The equation also provides an asymptotic expression for any mass transfer
17 process with a known memory function $g(t)$, which is easily calculated for a wide range
18 of sorption and diffusion processes. Conversely, it must be pointed out, the equations
19 developed by *Vereecken et al.* [1999] allow for time-varying velocity.

20 Second, (12) suggests that the density function of mass transfer rate coefficients
21 (whether from diffusion, nonequilibrium sorption, or a general density function of mass
22 transfer processes) is available directly and analytically from breakthrough data. In fact,

1 if (12) is treated as an integral equation where $b(\alpha)$ is an unknown, the density function
 2 $b(\alpha)$ may be directly calculated using the inverse Laplace transform. If the medium is
 3 initially free of tracer, then $c_0 = 0$ and the density function $b(\alpha)$ is given analytically by
 4 the Bromwich integral:

$$5 \quad b(\alpha) = \frac{1}{t_0 m_0 \alpha^2 (2\pi i)} \int_{Br} c(x=L, t) e^{-\alpha t} dt = \frac{1}{t_0 m_0 \alpha^2} \text{Lap}^{-1} \{ c(x=L, t) \} \quad (13)$$

6 where i is the unit imaginary number; and Br represents the Bromwich contour [see, e.g.,
 7 *LePage*, 1961, p. 319-320]. A similar equation may be easily constructed for the case of
 8 non-zero initial conditions and continuous flushing of tracer-free fluid, such as in a purge
 9 experiment. Unfortunately, the practical use of (13) is limited by the conditions that we
 10 can only use the late-time breakthrough data, and that any errors in the data introduce
 11 numerical instabilities in the inverse Laplace transform. Nonetheless, (13) will allow us
 12 to determine certain important properties of the density function $b(\alpha)$.

13 For relatively simple cases (i.e., single rate mass transfer), the properties of (12)
 14 allow estimation of the rate coefficient and capacity coefficient directly from the BTC
 15 [also see *Vereecken et al.*, 1999]. For some more complex cases (e.g., gamma and
 16 power-law density functions), the properties of (12) will allow certain properties of the
 17 density function of rate coefficients to be determined. This will be discussed in the
 18 following sections.

1 2.3. Notes on the Density Function $b(\alpha)$

2 We add two notes regarding the density function $b(\alpha)$ before continuing. First, a
 3 useful definition is that of the 0th moment of the density function of rate coefficients:

4
$$\int_0^\infty b(\alpha) d\alpha = \beta_{tot} \quad (14)$$

5 where β_{tot} is commonly known as the capacity coefficient. The capacity coefficient is
 6 the ratio of mass in the immobile domain to mass in the mobile domain at equilibrium; in
 7 the absence of sorption it is the ratio of the two volumes.

8 Second, we note without derivation that the Laplace transform of the density
 9 function of rate coefficients is a particularly useful function by itself. This function is
 10 proportional to the mass fraction remaining in an immobile domain, where the initial
 11 conditions are uniform concentration in the immobile domain and the boundary condition
 12 on the immobile domain is zero concentration. The mass fraction remaining in the entire
 13 system (M/M_0) is therefore:

14
$$\frac{M(t)}{M_0} = \frac{\text{Lap}\{b(\alpha)\}}{1 + \beta_{tot}} = \frac{\int_0^\infty b(\alpha) e^{-\alpha t} dt}{1 + \beta_{tot}} \quad (15)$$

15 In other words, the mass fraction remaining is calculated simply by finding the Laplace
 16 transform of the density function $b(\alpha)$.

1 2.4. Mean Residence Time in Immobile Domain

2 One of the criteria for use of equation (12) is that the mean residence time in the
 3 immobile domain be much greater than the advection time. This sub-section outlines the
 4 calculation of this mean residence time, as well as providing an effective rate coefficient
 5 that may be used in an "equivalent" first-order model of mass transfer.

6 The residence time distribution in the immobile domain given a Dirac impulse at
 7 the surface is $g(t)/\beta_{tot}$. The mean residence time (or characteristic mass transfer time) is
 8 therefore

$$9 \quad t_\alpha = \frac{1}{\beta_{tot}} \int_0^\infty t g(t) dt \\ = \frac{1}{\beta_{tot}} \int_0^\infty t \int_0^\infty \alpha b(\alpha) e^{-\alpha t} d\alpha dt \\ = \frac{1}{\beta_{tot}} \int_0^\infty \frac{b(\alpha)}{\alpha} d\alpha \quad (16)$$

10 It can be shown [e.g., Cunningham and Roberts, 1998] that the zeroth, first, and second
 11 temporal moments of the BTC are the same for any density function of rate coefficients
 12 provided that the mean residence time in the immobile domain is the same. Therefore,
 13 the best effective rate coefficient (i.e., the one that yields the same zeroth, first, and
 14 second moments of the BTC) is the harmonic mean of the density function, since:

$$15 \quad \hat{\alpha}_H = \frac{1}{t_\alpha} = \beta_{tot} \left(\int_0^\infty \frac{b(\alpha)}{\alpha} d\alpha \right)^{-1} \quad (17)$$

1 Notably, the harmonic mean may be zero for some density functions, meaning that the
2 mean residence time in the immobile domain is infinite. Note that an infinite mean
3 residence time does not require infinite size or infinite capacity in the immobile domain.
4 The harmonic means for a number of density functions $b(\alpha)$ are shown in Table 1.

5 **3. Late-Time Behavior of BTCs**

6 In this section we will consider a number of examples of BTCs after a pulse
7 injection into a medium with zero initial concentration. Many of the functions developed
8 in this section are summarized in Table 1, as are several others not discussed here.

9 **3.1. Simple Example 1: First-Order Mass Transfer**

10 Consider the simplest case of mass transfer described by a single first-order rate
11 coefficient. The density function of rate coefficients is

12

13 $b(\alpha) = \beta_{tot} \delta(\alpha - \alpha_f)$ (18)

14 The memory function $g(t)$, given by applying (10) to (18), is

15 $g(t) = \alpha_f \beta_{tot} e^{-\alpha_f t}$ (19)

16

17 The resulting late-time approximation for concentration in the mobile domain (with
18 initial concentration of zero) is given by substituting (19) into (12):

19 $c = m_c t_{ad} \beta_{tot} \alpha_f^2 e^{-\alpha_f t}$ (20)

1 This solution displays the well-known behavior that late-time concentration is
 2 exponential with a semi-log slope $d(\ln c)/dt$ of $-\alpha_f$.

3 **3.2. Simple Example 2: Finite Spherical Blocks**

4 Consider the case of diffusion into finite spherical matrix blocks. *Haggerty and*
 5 *Gorelick* [1995] showed that a particular discrete density function of first-order rate
 6 coefficients results in a model that is mathematically identical, from the perspective of
 7 the mobile domain concentrations, to that of diffusion into and out of various matrix
 8 geometries. Using mathematics that is more similar to that presented in this paper,
 9 *Carrera et al.* [1998] make the same assertion. In the case of spherical blocks, the
 10 density function is

$$11 \quad b(\alpha) = \sum_{j=1}^{\infty} \frac{6\beta_{tot}}{j^2\pi^2} \delta_j \left(\alpha - j^2\pi^2 \frac{D_a}{a^2} \right) \quad (21)$$

12 where β_{tot} [-] is the capacity coefficient of the spherical blocks; D_a [T^{-1}] is the apparent
 13 diffusivity; and a [L] is the radius of the spherical blocks. This density function is a
 14 series of Dirac deltas with monotonically decreasing weight. The harmonic mean of (21)
 15 is the well-known linear driving force approximation 15 D_a/a^2 [e.g., *Glueckauf*, 1955],
 16 and the mean residence time in the spheres is therefore $t_a = a^2/15D_a$. The memory
 17 function is

$$18 \quad g(t) = \sum_{j=1}^{\infty} 6\beta_{tot} \frac{D_a}{a^2} \exp \left(- j^2\pi^2 \frac{D_a}{a^2} t \right) \quad (22)$$

1 Readers familiar with diffusion in spherical geometry will recognize (22) as
2 proportional to the mass flux out of spheres initially saturated with a uniform solute
3 concentration and with a boundary concentration of zero. [e.g., Crank, 1975, p. 91;
4 Grathwohl et al., 1994].

5 The resulting late-time approximation for concentration in the mobile domain
6 (with initial concentration of zero) is given by substituting (22) into (12):

$$7 \quad c = m_0 t_{ad} \beta_{tot} \left(\frac{D_a}{a^2} \right)^2 \sum_{j=1}^{\infty} 6j^2 \pi^2 \exp \left(-j^2 \pi^2 \frac{D_a t}{a^2} \right) \quad (23)$$

8 From this expression, we can see that the late-time concentration is exponential;
9 therefore, on a double-log plot, the late-time slope will approach ∞ shortly after the mean
10 residence time in the immobile domain ($t_\alpha = a^2/15D_a$) is reached.

11 Figure 1 shows the full solution to the advection-dispersion-mass transfer
12 (ADMT) equations and the late-time approximation. The ADMT equations were solved
13 using STAMMT-L [Haggerty and Reeves, 1999] for $m_0 = 1 \times 10^4 \text{ s kg m}^{-3}$;
14 $t_{ad} = 1 \times 10^4 \text{ s}$; $D_a/a^2 = 1 \times 10^{-8} \text{ s}^{-1}$; $\beta_{tot} = 1$; and a Peclet number of 1000. All
15 concentrations have been nondimensionalized by the terms in front of the infinite series
16 in (23).

17 From Figure 1 we make four points. First, the approximation very accurately
18 represents the late-time behavior of the ADMT solution, but obviously does not contain
19 the advective-dispersive peak. We can see in the figure that the late-time approximation
20 is valid when $t \gg t_{ad}$ provided that $t_\alpha \gg t_{ad}$.

1 Second, the late-time behavior demonstrates the well-known 3/2 slope for matrix
2 diffusion [e.g., *Hadermann and Heer*, 1996], which ends when $tD_a/\alpha^2 > 1$. As long as
3 the block size α is large enough (or D_a small enough) that $tD_a/\alpha^2 \ll 1$ over the entire
4 time of a tracer test, then the slope remains 3/2. In such a case it would not be possible
5 to estimate the value of D_a/α^2 from the BTC. The limiting case of "infinite" matrix
6 blocks is given in Table 1, for $c \sim dg/dt \sim t^{3/2}$. Note that the harmonic mean rate
7 coefficient for this case is zero, meaning that the mean residence time for very large
8 blocks approaches infinity.

9 Third, the location of the BTC peak in the ADMT solution may lie anywhere on
10 the late-time approximation curve, dependent on the relative values of t_{ad} and D_a/α^2 .

11 Last, we note that it is possible to estimate both β_{tot} and D_a/α^2 by using the late-
12 time approximation as a type-curve, if the break in slope is present. The capacity
13 coefficient β_{tot} would be estimated from the vertical shift, while D_a/α^2 would be
14 estimated from the horizontal shift.

15 3.3. Gamma Density Function of First-Order Rate Coefficients

16 Gamma density functions of rate coefficients have been used to represent
17 multirate mass transfer in several papers. *Cunningham et al.* [1997] developed the
18 mathematics of a gamma density function of diffusion rate coefficients, while *Werth et*
19 *al.* [1997] applied this model successfully to several mass-fraction-remaining data sets.
20 *Connaughton et al.* [1993] used a gamma density function of first-order rate coefficients
21 to model release of naphthalene from soil, while *Pedit and Miller* [1994] employed a
22 gamma density function of first-order rate coefficients to examine diuron sorption. Other

1 examples include *Ahn et al.* [1996]; *Chen and Wagenet* [1997]; *Culver et al.* [1997];
 2 *Sahoo and Smith* [1997]; *Deitsch et al.* [1998]; *Kauffman et al.* [1998]; *Lorden et al.*
 3 [1998], and *Stager and Perram* [1999]. The method we are using is applicable to both
 4 types of density functions, and the key relationships for both are given in Table 1.
 5 Although the early time behavior will differ between gamma density functions of first-
 6 order and diffusion rate coefficients, the late-time slope will be identical for the same
 7 value of η .

8 The gamma density function of first-order rate coefficients is

9

$$b(\alpha) = \frac{\beta_{tot}}{\gamma^\eta \Gamma(\eta)} \alpha^{\eta-1} e^{-\alpha/\gamma} \quad (24)$$

10 where γ [T^{-1}] is the scale parameter and η [-] is the shape parameter. The harmonic mean
 11 of (24) is 0 if η is less than 1, a fact that is of particular importance for applications. As
 12 a consequence, the mean residence time in the immobile domain would be infinite.
 13 (These facts are also true for gamma density functions of diffusion rate coefficients.) If
 14 η is greater than 1, the harmonic mean of (24) is $(\eta-1)\gamma$.

15 The memory function is

16

$$g(t) = \beta_{tot} \frac{\partial}{\partial t} (\gamma t + 1)^{-\eta} \quad (25)$$

17 Therefore, the late-time concentration in the fracture is given by

18

$$c = m_c J_{ad} \beta_{tot} \gamma^2 \frac{\eta(\eta+1)}{(\gamma t + 1)^{\eta+2}} \quad (26)$$

19 Note that when $\gamma t \gg 1$ the BTC follows a power-law:

$$1 \quad c \sim t^{-\eta-2} \quad (27)$$

2 The same late-time power-law behavior is also exhibited with a density function of
 3 diffusion rate coefficients. Note that a power-law behavior ($c \sim t^k$) with $k < 3$ would
 4 indicate an infinite second (and higher) temporal moment and an infinite mean residence
 5 time in the immobile domain.

6 Figure 2 shows the late-time approximation in (26) nondimensionalized by the
 7 transport terms. We have normalized time by the mass transfer rate γ . Figure 2 also
 8 shows a solution to the ADMT equations with STAMMT-L (*Haggerty and Reeves, 1999*)
 9 for $m_0 = 1 \times 10^4 \text{ s kg m}^{-3}$; $t_{ad} = 1 \times 10^4 \text{ s}$; $\gamma = 1 \times 10^{-4} \text{ s}^{-1}$; $\eta = 0.5$; $\beta_{tot} = 1$; and a Peclet
 10 number of 1000.

We see from (27) and Figure 2 that the late-time double-log slope of concentration will be $-(\eta+2)$. For comparison to published values, *Connaughton et al.* [1993] estimated values of η in the range of 0.17 to 0.37 for a gamma density function of first-order rate coefficients, while *Pedit and Miller* [1994] estimated $\eta = 0.11$ from their experiments; *Culver et al.* [1997] estimated $\eta = 0.023$ to 0.054 for their column experiments; *Deitsch et al.* [1998] estimated η from 0.092 to 350 in 15 experiments with different materials, with the majority having η below 1. *Kauffman et al.* [1998] estimated $\eta = 0.60$ and 0.84 in two column experiments. *Werth et al.* [1997] found values of η equal to approximately 0.5 for a gamma density function of diffusion rate coefficients. Note that almost all of these estimated η (i.e., those below 1) will lead to an infinite mean residence time within the immobile domain. Consequently, the variance of

1 the breakthrough times will be infinite with these models. Late-time behavior associated
 2 with gamma density functions is discussed further in Section 4.2.

3 **3.4. Lognormal Density Function of Diffusion Rate Coefficients**

4 Lognormal density functions of rate coefficients have also been used to represent
 5 mass transfer in natural systems. *Pedit and Miller* [1994]; *Backes et al.* [1995];
 6 *Haggerty* [1995]; *Culver et al.* [1997]; *McLaren et al.* [1998] all used a lognormal
 7 density function of first-order rate coefficients to model uptake and release of sorbing
 8 solutes in soils. *Pedit and Miller* [1995] and *Haggerty and Gorelick* [1998] used a
 9 lognormal density function of diffusion rate coefficients to model diffusion of sorbing
 10 solutes in soils. As is true for the gamma density functions of rate coefficients, the
 11 behavior of both lognormal models is very similar, especially at late time and large
 12 variances. In our analysis here we will employ only a density function of diffusion rate
 13 coefficients:

$$14 \quad b^* \left(\frac{D_a}{a^2} \right) = \frac{\beta_{tot}}{\sqrt{2\pi} \sigma \frac{D_a}{a^2}} \exp \left\{ - \frac{\left[\ln \left(\frac{D_a}{a^2} \right) - \mu \right]^2}{2\sigma^2} \right\} \quad (28)$$

15 The equivalent density function of first-order rate coefficients is given by *Haggerty and*
 16 *Gorelick* [1998]:

$$1 \quad b(\alpha) = \sum_{j=1}^{\infty} \frac{8\beta_{tot}}{\sqrt{2\pi^5(2j-1)^2\sigma^2\alpha}} \exp\left(-\frac{\left\{\ln\left[\frac{4\alpha}{(2j-1)^2\pi^2}\right] - \mu\right\}^2}{2\sigma^2}\right) \quad (29)$$

2 The harmonic mean of (29) is $3\exp(\mu-\sigma^2/2)$. Consequently, the effective rate coefficient
 3 is approximately $0.22\sigma^2$ orders of magnitude smaller than the geometric mean. For large
 4 σ , the effective rate coefficient is approximately zero and the mean residence time in the
 5 immobile domain approaches infinity. In the limit of very large σ , the density function is
 6 log-uniform and is equivalent to a power-law density function with $\sim \alpha^{-1}$. As we shall
 7 see in the following sections, this corresponds to a late-time BTC of $\sim t^2$.

8 The Laplace transform of (29) must be done numerically. The result may then be
 9 inserted into (12). After taking the second derivative in time (numerically), the late-time
 10 approximation for a concentration BTC is shown in Figure 3 for various values of σ .

11 The time axis of Figure 3 is normalized by the geometric mean of (24), and concentration
 12 is normalized the same as previously. Figure 3 also shows the solution to the ADMT
 13 equations in the presence of a lognormal density function of diffusion rate coefficients.

14 The ADMT equations were solved using STAMMT-L [Haggerty and Reeves, 1999] for
 15 $m_0 = 1 \times 10^4 \text{ s kg m}^{-3}$; $t_{ad} = 1 \times 10^4 \text{ s}$; $e^{-\mu} = 1 \times 10^{-4} \text{ s}^{-1}$; $\sigma = 5$; $\beta_{tot} = 1$; and a Peclet
 16 number of 1000. The discrepancy at late time is due to numerical error in the series of
 17 numerical steps for the late-time approximation; however, the late-time slopes are
 18 correct. Note that the late-time slopes for the lognormal distribution lie between 2 and 3
 19 for a large range of time, provided that σ is greater than approximately 3.

1 Published values of σ for lognormal distributions of rate coefficients are typically
2 larger than 3 [e.g., *Pedit and Miller*, 1994, 1995; *Culver et al.*, 1997; *Haggerty and*
3 *Gorelick*, 1998; *Haggerty et al.*, in review], suggesting that mass transfer rate coefficients
4 have large variability in natural media. With such large values of σ , we would expect to
5 see late-time slopes on double-log BTCs after a pulse-injection between 2 and 3.

6 **3.5. Power Law Density function of First-Order Rate Coefficients**

7 An alternative density function that has been less commonly used to describe
8 mass transfer in groundwater and soils is a power-law density function. *Hatano and*
9 *Hatano* [1998] used a power-law density function of waiting times in the context of a
10 continuous-time random walk to model the sorption of radionuclides in a column
11 experiment. Power-law density functions of waiting times have been used in statistical
12 physics to describe anomalous transport behavior [e.g., *Bouchard and Georges*, 1990;
13 *Scher et al.*, 1991]. Frequently such density functions arise from diffusion or rate-limited
14 sorption on a fractal geometry. A particular advantage of a power-law distribution,
15 within the context of this work, is that it allows us to investigate power-law BTC
16 behavior for a larger range of late-time slopes.

17 As with a gamma density function it is possible to define both a density function
18 of first-order rate coefficients and an equivalent density function of diffusion rate
19 coefficients. Again, although the early time behavior will differ for power-law density
20 functions of first-order and diffusion rate coefficients, the late-time slope will be
21 identical for the same value of k . For the sake of brevity, we show only the power-law
22 density function of first-order rate coefficients.

1 A truncated power-law density function may be written as follows:

2

$$b(\alpha) = \frac{\beta_{tot}(k-2)}{\alpha_{max}^{k-2} - \alpha_{min}^{k-2}} \alpha^{k-3}, \quad k > 0 \text{ and } k \neq 2, \quad \alpha_{min} \leq \alpha \leq \alpha_{max} \quad (30a)$$

3 where α_{max} [T^{-1}] is the maximum rate coefficient; α_{min} [T^{-1}] is the minimum rate
4 coefficient; and k is the exponent. The value of α_{min} may be zero if $k > 2$. The reason for
5 choosing to write the power-law as $k-3$ will become apparent shortly. If $k = 2$, the
6 density function may be written

7

$$b(\alpha) = \frac{\beta_{tot}}{\ln\left(\frac{\alpha_{max}}{\alpha_{min}}\right)} \alpha^{-1} \quad (30b)$$

8 The late-time concentration in the mobile domain is

9

$$c = \frac{m_0 t_{ad} \beta_{tot} (k-2)}{\left(\alpha_{max}^{k-2} - \alpha_{min}^{k-2}\right)} \int_{\alpha_{min}}^{\alpha_{max}} \alpha^{k-1} e^{-\alpha t} d\alpha, \quad k > 0 \text{ and } k \neq 2 \quad (31)$$

10 For arbitrary (non-integer) values of k , (31) must in general be evaluated
11 numerically. However, the most important point about (31) is that

12

$$c \sim t^{-k}, \quad \alpha_{max}^{-1} \ll t \ll \alpha_{min}^{-1} \quad (32)$$

13 Expressed in words, the slope of the BTC is k for times much greater than α_{max}^{-1} and
14 much less than α_{min}^{-1} for all values of k . At times greater than α_{min}^{-1} the slope goes to ∞ .

1 It is possible to present closed form solutions for many specific cases of (31); we
 2 will provide the solutions for the cases $k = 1$, $k = 2$, and $k = 3$. First, let us define three
 3 other variables in terms of α_{\max} and α_{\min} :

4 $\tau = \alpha_{\max} t$ (33a)

5 $\lambda_t = \frac{\alpha_{\max}}{\alpha_{\min}}$ (33b)

6 $\alpha_p^2 = \begin{cases} \frac{\alpha_{\max}^2}{1 - \lambda_t^{2-k}}, & k \neq 2 \\ \frac{\alpha_{\max}^2}{\ln(\lambda_t)}, & k = 2 \end{cases}$ (33c)

7 Note that α_p is a function of α_{\max} , α_{\min} , and k , and is used for the purpose of simplifying
 8 the following equations only.

9 Using these variables, the late-time concentration for $k = 1$ is therefore

10 $c = m_0 t_{ad} \beta_{tot} \alpha_p^2 \left(e^{-\tau/\lambda_t} - e^{-\tau} \right) \tau^{-1}$ (34)

11 If $k = 2$, then the density function is log-uniform, and the late-time concentration is

12 $c = m_0 t_{ad} \beta_{tot} \alpha_p^2 \left[e^{-\tau/\lambda_t} \left(\frac{\tau}{\lambda_t} + 1 \right) - e^{-\tau} (\tau + 1) \right] \tau^{-2}$ (35)

13 If $k = 3$, then the density function is uniform, and the late-time concentration is

14 $c = m_0 t_{ad} \beta_{tot} \alpha_p^2 \left[e^{-\tau/\lambda_t} \left(\frac{\tau^2}{\lambda_t^2} + \frac{2\tau}{\lambda_t} + 2 \right) - e^{-\tau} (\tau^2 + 2\tau + 2) \right] \tau^{-3}$ (36)

1 From the above equations we see that a family of curves is required for each value of k
2 since both α_{min} and α_{max} appear in all equations. However, inspection of the equations
3 indicates that the curves for each value of k will be identical until t approaches α_{min}^{-1} .

4 The harmonic mean of the density function (30a) and (30b) is

$$\ln(\lambda_t) \frac{\alpha_{min} \lambda_t}{\lambda_t - 1}, \quad k = 2$$

5
$$\hat{\alpha}_H = \frac{\alpha_{max}}{\ln(\lambda_t)}, \quad k = 3 \quad (37)$$

$$\alpha_{min} \frac{(k-3)}{(k-2)} \frac{\lambda_t^{k-2} - 1}{\lambda_t^{k-3} - 1}, \quad \text{otherwise}$$

6 Approximations may be made to (37) that are useful in understanding what controls the
7 harmonic mean of the distribution. These approximations are given in Table 2. Note
8 again that the mean residence time in the immobile domain is simply the inverse of $\hat{\alpha}_H$.

9 We make two points in regard to (37) and Table 2, and leave further discussion of
10 late-time behavior associated with power-law density functions to Section 4.2. First, if
11 the late-time slope of the BTC is less than 3 (i.e., $k < 3$), then the harmonic mean is
12 controlled by α_{min} . However, if the late-time behavior of the BTC remains power-law
13 until the end of the experiment, the parameter α_{min} cannot be estimated from a BTC.
14 Consequently, the harmonic mean (and therefore the mean residence time in the
15 immobile domain) cannot be estimated if the BTC remains power-law until the end of
16 the experiment with a slope less than 3.

17 Second, if $k < 3$ and $\alpha_{min} = 0$, then the harmonic mean is 0. Therefore, if a
18 BTC has a late-time slope of $k < 3$, and the behavior is due to mass transfer, this may

1 indicate an infinite mean residence time in the immobile domain. It also causes the
2 second and higher temporal moments of the BTC to be infinite.

3 Note that there is nothing that physically precludes a late-time slope between 2
4 and 3 being maintained to infinite time (i.e., $2 < k < 3$ as $t \rightarrow \infty$). A slope of $k \leq 2$ to
5 infinite time, however, would require an infinitely large immobile domain (i.e., infinite
6 capacity). Therefore, a slope of $k \leq 2$ cannot be maintained for infinite time (for this
7 reason, $k = 3/2$ is possible with diffusion, but only until a time of $\sim a^2/D_a$).

8 The late-time behavior of concentration, as given by (34) - (36) is shown in
9 Figure 4 for $\alpha_{min} = 10^{-5} \alpha_{max}$. Figure 4 also shows the solution to the ADMT equations
10 in the presence of a power-law density function of rate coefficients. The ADMT
11 equations were solved using STAMMT-L [Haggerty and Reeves, 1999] for $m_0 = 1 \text{ s kg}$
12 m^{-3} ;

13 $t_{ad} = 1 \text{ s}$; $\alpha_{max} = 1 \text{ s}^{-1}$; $\alpha_{min} = 1 \times 10^{-5} \text{ s}^{-1}$; $k = 1$; $\beta_{tot} = 1$; and a Peclet number of 1000.

14 3.6. Summary of Late-Time Slopes

15 Figure 5 provides a summary of late-time slopes for several of the models
16 presented. Late-time slopes are given versus nondimensional time. Note that a BTC
17 with advection and dispersion will mask some portion of the slopes shown in this figure
18 at earlier times. The slopes given in Figure 5 will only be present when $t \gg t_{ad}$. A
19 power-law slope is a constant at late-time, such as provided by the gamma and power-
20 law density functions. Note that the conventional diffusion model is equivalent to the
21 lognormal density function with $\sigma = 0$. The slope in the conventional model is 3/2 until

1 approximately the mean residence time in the immobile domain ($\sigma^2/3D_a$ for 1-D
2 diffusion). Note that the lognormal density function with larger σ cannot provide a true
3 power-law BTC, but can hold the slope relatively constant over a long time. All
4 lognormal density functions will approach an infinite slope as time goes to infinity.

5 **4. Applications to Tracer Tests and Discussion**

6 **4.1. WIPP Tracer Tests**

7 Figure 6a shows data and confidence intervals from two single-well injection-
8 withdrawal (SWIW) tracer tests conducted in the Culebra Dolomite Member of the
9 Rustler Formation at the Waste Isolation Pilot Plant (WIPP) Site in southeastern New
10 Mexico. The Culebra is a 7-m-thick, variably fractured dolomite, and is a potential
11 pathway to the accessible environment in the event of a radionuclide release from the
12 WIPP. These two tests were performed in the central well at two multi-well sites,
13 designated H-11 and H-19. The SWIW tests consisted of the consecutive injection of
14 one or more slugs of conservative tracers into the Culebra Dolomite, followed by the
15 injection of a Culebra brine chaser (containing no tracer), and then by a resting period of
16 approximately 6.5×10^4 s (18 h). The tracers were then removed from the formation by
17 pumping on the same well until concentration was close to or below detection levels.
18 The total residence time (i.e., t_{ad}) of the slug in the formation was approximately $9.0 \times$
19 10^4 s (25 h). Details of the tracer tests are given in *Meigs and Beauheim* [in review] and
20 in *Meigs et al.* [in press]. Interpretation of the SWIW tests by *Haggerty et al.* [in review]
21 suggest that the late-time behavior of the BTC is due to multiple rates of mass transfer.

1 It is clear that neither heterogeneity nor tracer drift alone can be responsible for the
2 observed behavior, though a combination of the two may explain some fraction of it
3 [Meigs et al., in press; Lesoff and Konikow, 1997].

4

5 The SWIW data in Figure 6a display late-time slopes that are approximately
6 constant over several hundred hours. The slopes at all times for both BTCs are given in
7 Figure 6b, which was calculated using a 5-point, moving-window average. As can be
8 seen from both figures, the late-time behavior of both BTCs is essentially power-law.

9 The H11-1 BTC has a slope of about 2.1 after 3×10^5 s (83 h). The slope of the H11-1
10 BTC appears to become more negative after about 3×10^6 s (830 h), but this may be due
11 to a 70% increase in the pumping rate at that time. In addition, the accuracy of the data
12 is relatively low after 3×10^6 s, making slope calculations uncertain. The H19S1-1 BTC
13 has a constant slope of about 2.3 from 6×10^5 s (170 h) to the end of the test. Note that
14 conventional (single-rate) diffusion can only provide a constant late-time slope of 3/2,
15 which is shown for comparison in Figure 6a.

16 The late-time behavior of the SWIW tests was interpreted by Haggerty et al. [in
17 review] using a lognormal density function of diffusion rate coefficients (D_a/a^2). As
18 shown in that paper, a lognormal density function does an excellent job of representing
19 the entire BTC (with $\sigma = 3.55$ for H11-1 and $\sigma = 6.87$ for H19S1-1). However, based on
20 the BTC data alone it is not possible to rule out other density functions of rate
21 coefficients, including a gamma density function or a power-law density function.

1 4.2. Implications of Power-Law BTC Behavior

2 We note again that both the gamma and power-law density functions result in
3 power-law BTCs at late time. The conventional diffusion model also causes power-law
4 BTCs with a slope of $3/2$ prior to $t \sim \alpha^2/D_a$. There are four important scenarios for such
5 power-law behavior.

6 *CASE 1 – Power-law behavior to infinite time and $k \leq 3$:* The first scenario is that
7 the BTC behaves as a power law over all time (i.e., the slope of the BTC would be
8 power-law to infinite time) and the slope is less than 3. It is important to note that (1)
9 this is physically possible provided that the slope k is also greater than 2; and (2) several
10 papers effectively invoke Case 1 by assuming a gamma density function and finding
11 estimates of η less than 1 [e.g., *Connaughton et al.*, 1993; *Pedit and Miller*, 1994; *Culver*
12 *et al.*, 1997; *Werth et al.*, 1997; *Deitsch et al.*, 1998; *Kauffman et al.*, 1998; *Lorden et al.*,
13 1998]. In Case 1, the mean residence time in the immobile domain must be infinite.
14 Consequently, there can be no effective single-rate model that is equivalent to the
15 multirate model in the way that a single-rate first-order model is approximately
16 equivalent to a conventional single-rate diffusion model. No single-rate (either first-
17 order or diffusion) model can yield the same second or higher temporal moments as the
18 multirate model. In fact, any single-rate model (either first-order or diffusion) fit to data
19 will have parameters that are a function of the experimental observation time (i.e., the
20 experiment length).

21 *CASE 2 – Power-law behavior longer than experimental time-scale and $k \leq 3$:*
22 The second scenario is that the power-law behavior ends at a particular time that is

1 beyond the experimental observation time, and the slope is less than 3. In this case, the
2 mean residence time in the immobile domain cannot be ascertained from the
3 experimental data alone. In other words, it is impossible, based solely on the BTC data,
4 to estimate an effective rate coefficient: the effective rate coefficient could be either
5 undefined (as in Case 1) or simply longer than the inverse of the experimental time.

6 If the slope k is less than 2, then the power-law behavior either must end at some
7 time or the slope must steepen to greater than 2. Such is the case with conventional
8 diffusion and a slope of 3/2. Because the immobile domain cannot be infinitely thick, the
9 power-law behavior with k less than 2 must end at some time. However, without
10 information external to the tracer test data, the time at which the power-law behavior
11 ends (and therefore the mean residence time in the immobile domain) cannot be known.

12 *CASE 3 – Power-law behavior ends within experimental time-scale:* The third
13 scenario is that the power-law behavior ends within the experimental observation time.
14 An example of this is the conventional diffusion model with a slope of 3/2 at
15 intermediate time. In this case, an effective rate coefficient or mean residence time in the
16 immobile domain can be estimated. The mean residence time will be larger for smaller
17 slopes, and for very small slopes will approach the inverse of the time at which the
18 power-law behavior ends. Note that Case 3 cannot be modeled by a gamma density
19 function because a gamma density function does not allow for an end to the power-law
20 behavior.

21 *CASE 4 – Power-law behavior with $k > 3$:* The fourth scenario is that the BTC
22 has a slope greater than 3. In this case the mean residence time can be estimated even if
23 the power-law behavior extends to infinite time. This is because the harmonic mean of a

1 power-law density function is non-zero and dominated by the value of α_{\max} , provided that
2 $k > 3$.

3 Which scenario do the WIPP SWIW tracer tests fall into? Based on the BTC data
4 alone, H19S1-1 must be either Case 1 or Case 2. Since the power-law behavior extends
5 to the end of the data set, it is not possible to estimate the mean residence time of the
6 immobile domain. We know only that the mean residence time must be at least the
7 inverse of the experimental time (i.e., $\sim 1.9 \times 10^6$ s). H11-1, on the other hand, may be
8 Case 3. If the marked change in slope at approximately 3×10^6 s is not primarily due to
9 the increase in pumping rate, then H11-1 is Case 3. However, if this is an artifact of the
10 increase in pumping rate, then H11-1 may be Case 1 or 2. Given the data uncertainty
11 after approximately 2×10^6 s (560 h) and the fact that we have not investigated the case
12 of time-varying pumping rate, we remain uncertain as to which case H11-1 falls under.

13 **5. Conclusions**

14 With improvements in experimental and analytical techniques, breakthrough
15 curves (BTCs) are now available from many laboratory and field experiments with
16 several orders of magnitude of data in both time and concentration. The late-time
17 behavior of BTCs is critically important for the evaluation of rate-limited mass transfer,
18 especially if discrimination between different models of mass transfer is desired.
19 Double-log plots of BTCs are particularly helpful and commonly yield valuable
20 information about mass transfer.

21 We have six primary conclusions.

1 First, we derived a simple analytical expression for late-time BTC behavior in the
2 presence of mass transfer. Equation (12) gives the late-time concentration for any linear
3 rate-limited mass transfer model for either zero-concentration or equilibrium initial
4 conditions. The expression requires the advection time-scale, the zeroth moment of the
5 injection pulse, the initial concentration in the system, and the memory function $g(t)$ be
6 known. Note that caution is advised in using (12) if the variance of t_{ad} may be large
7 (such as in a strongly heterogeneous velocity field).

8 Second, the memory function $g(t)$ is proportional to the residence time
9 distribution in the immobile domain given a unit impulse at the surface of the immobile
10 domain. This memory function is simply the derivative of the Laplace transform of the
11 density function of rate coefficients describing the immobile domain. Consequently, the
12 late-time concentration is proportional to the first or second derivative of the Laplace
13 transform of the density function of rate coefficients.

14 Third, the effective rate coefficient that yields the same zeroth, first, and second
15 BTC temporal moments as does the full density function is the harmonic mean of the
16 density function of rate coefficients. However, for any density function of rate
17 coefficients with power-law α^{k-3} as $\alpha \rightarrow 0$ and where $k \leq 3$, the harmonic mean is zero.
18 Consequently the mean residence time in the immobile domain is infinite and there is no
19 single effective rate coefficient. This applies both to density functions of diffusion rate
20 coefficients and density functions of first-order rate coefficients. Many such
21 distributions have been invoked in the literature.

1 Fourth, if the BTC (after a pulse injection) goes as $\sim t^k$ as $t \rightarrow \infty$, then the
2 underlying density function of rate coefficients must be $\sim \alpha^{k-3}$ as $\alpha \rightarrow 0$. This holds for
3 density functions of both first-order and diffusion rate coefficients. For a BTC from a
4 medium with initially non-zero but equilibrium concentrations, the equivalent BTC goes
5 as t^{1-k} .

6 Fifth, if the slope of a BTC (after a pulse injection) goes to k as
7 $t \rightarrow \infty$, and $k \leq 3$, then the mean residence time in the immobile domain is infinite. (This
8 is a corollary to the third and fourth conclusions.) Consequently there is no single
9 effective rate coefficient in this medium. A second consequence is that any single-rate
10 (either diffusion or first-order) rate coefficient estimated from the BTC will be a function
11 of experimental observation time. Again, for a BTC from a medium with initially non-
12 zero but equilibrium concentrations, then the equivalent BTC goes as t^{k+1} .

13 Sixth, if a BTC exhibits power-law behavior ($c \sim t^k$) to the end of the
14 experiment, then one of two cases must exist. If $k \leq 3$ then the mean residence time (and
15 effective rate coefficient) cannot be estimated from the BTC. The mean residence time
16 must be at least the experimental observation time and could be infinite. If $k > 3$ then the
17 mean residence time (and its inverse, the effective rate coefficient) can be estimated.

18

References

19 Ahn, I. S., L. W. Lion, and M. L. Shuler, Microscale-based modeling of polynuclear
20 aromatic hydrocarbon transport and biodegradation in soil, *Biotechnol. Bioeng.*,
21 51(1), 1-14, 1996.

1 Albery, W. J., P. N. Bartlett, C. P. Wilde, and J. R. Darwent, A general model for
2 dispersed kinetics in heterogeneous systems, *J. Am. Chem. Soc.*, 107(7), 1854-1858,
3 1985.

4 Backes, E. A., R. G. McLaren, A. W. Rate, and R. S. Swift, Kinetics of cadmium and
5 cobalt desorption from iron and manganese oxides, *Soil Sci. Soc. Am. J.*, 59(3), 778-
6 785, 1995.

7 Berkowitz, B., and H. Scher, Anomalous transport in random fracture networks, *Phys.*
8 *Rev. Lett.*, 79(20), 4038-4041, 1997.

9 Bouchaud, J.-P., and A. Georges, Anomalous diffusion in disordered media: Statistical
10 mechanisms, models and physical applications, *Phys. Rep.*, 195(4-5), 127-293,
11 1990.

12 Brusseau, M. L., R. E. Jessup, and P. S. C. Rao, Modeling the transport of solutes
13 influenced by multiprocess nonequilibrium, *Water Resour. Res.*, 25(9), 1971-1988,
14 1989.

15 Cameron, D. R., and A. Klute, Convective-dispersive solute transport with a combined
16 equilibrium and kinetic adsorption model, *Water Resour. Res.*, 13(1), 183-188,
17 1977.

18 Carrera, J., X. Sánchez-Vila, I. Benet, A. Medina, G. Galarza, and J. Guimerà, On matrix
19 diffusion: Formulations, solution methods and qualitative effects, *Hydrogeol. J.*,
20 6(1), 178-190, 1998.

21 Chen, W., and R. J. Wagenet, Solute transport in porous media with sorption-site
22 heterogeneity, *Environ. Sci. Technol.*, 29(11), 2725-2734, 1995.

- 1 Chen, W., and R. J. Wagenet, Description of atrazine transport in soil with heterogeneous
- 2 nonequilibrium sorption, *Soil Sci. Soc. Am. J.*, 61(2), 360-371, 1997.
- 3 Coats, K. H., and B. D. Smith, Dead-end pore volume and dispersion in porous media,
- 4 *Soc. Pet. Eng. J.*, 4(1), 73-84, 1964.
- 5 Connaughton, D. F., J. R. Stedinger, L. W. Lion, and M. L. Shuler, Description of time-
- 6 varying desorption kinetics: Release of naphthalene from contaminated soils,
- 7 *Environ. Sci. Technol.*, 27(12), 2397-2403, 1993.
- 8 Crank, J., *The Mathematics of Diffusion*, 2nd ed., Oxford Univ. Press, New York, 1975.
- 9 Culver, T. B., S. P. Hallisey, D. Sahoo, J. J. Deitsch, and J. A. Smith, Modeling the
- 10 desorption of organic contaminants from long-term contaminated soil using
- 11 distributed mass transfer rates, *Environ. Sci. Technol.*, 31(6), 1581-1588, 1997.
- 12 Cunningham, J. A., C. J. Werth, M. Reinhard, and P. V. Roberts, Effects of grain-scale
- 13 mass transfer on the transport of volatile organics through sediments. 1. Model
- 14 development, *Water Resour. Res.*, 33(12), 2713-2726, 1997.
- 15 Cunningham, J. A., and P. V. Roberts, Use of temporal moments to investigate the
- 16 effects of nonuniform grain-size distribution on the transport of sorbing solutes,
- 17 *Water Resour. Res.*, 34(6), 1415-1425, 1998.
- 18 Deitsch, J. J., J. A. Smith, M. B. Arnold, and J. Bolus, Sorption and desorption rates of
- 19 carbon tetrachloride and 1,2-Dichlorobenzene to three organobentonites and a
- 20 natural peat soil, *Environ. Sci. Technol.*, 32(20), 3169-3177, 1998.
- 21 Eikenberg, J., E. Hoehn, Th. Fierz, and U. Frick, *Grimsel Test Site: Preparation and*
- 22 *performance of migration experiments with radioisotopes of sodium, strontium and*
- 23 *iodine*, Paul Scherrer Inst., Würenlingen, PSI-Bericht No. 94-11, 1994.

- 1 Farrell, J., and M. Reinhard, Desorption of halogenated organics from model solids,
- 2 sediments, and soil under unsaturated conditions. 2. Kinetics, *Environ. Sci. Technol.*,
- 3 28(1), 63-72, 1994.
- 4 Fong, F. K., and L. A. Mulkey, Solute transport in aggregated media: Aggregated size
- 5 distribution and mean radii, *Water Resour. Res.*, 26(6), 1291-1303, 1990.
- 6 Glueckauf, E., Theory of chromatography. Part 10: Formulae for diffusion into spheres
- 7 and their application to chromatography, *Trans. Faraday Soc.*, 51(11), 1540-1551,
- 8 1955.
- 9 Grathwohl, P., W. Pyka, and P. Merkel, Desorption of organic pollutants (PAHs) from
- 10 contaminated aquifer material, *Transport and Reactive Processes in Aquifers*, edited
- 11 by T. Dracos and F. Stauffer, Balkema, Brookfield, VT, 469-474, 1994.
- 12 Hadermann, J., and W. Heer, The Grimsel (Switzerland) migration experiment:
- 13 Integrating field experiments, laboratory investigations and modelling, *J. Contam.*
- 14 *Hydrol.*, 21(1-4), 87-100, 1996.
- 15 Haggerty, R., *Aquifer Remediation in the Presence of Rate-Limited Mass Transfer*, PhD
- 16 Dissertation, Stanford University, Stanford, CA, 1995.
- 17 Haggerty, R., and S. M. Gorelick, Multiple-rate mass transfer for modeling diffusion and
- 18 surface reactions in media with pore-scale heterogeneity, *Water Resour. Res.*,
- 19 31(10), 2383-2400, 1995.
- 20 Haggerty, R., and S. M. Gorelick, Modeling mass transfer processes in soil columns with
- 21 pore-scale heterogeneity, *Soil Sci. Soc. Am. J.*, 62(1), 62-74, 1998.
- 22 Haggerty, R., and P. Reeves, *STAMMT-L: Solute Transport and Multirate Mass*
- 23 *Transfer, User's Manual*, Sandia National Laboratories, Albuquerque, NM, 1999.

- 1 Haggerty, R., S. W. Fleming, L. C. Meigs, and S. A. McKenna, Tracer tests in a
- 2 fractured dolomite. 3. Analysis of mass transfer in single-well injection-withdrawal
- 3 tests, submitted to *Water Resour. Res.*, December, 1998, accepted pending revisions
- 4 to be completed.
- 5 Hatano, Y., and N. Hatano, Dispersive transport of ions in column experiments: An
- 6 explanation of long-tailed profiles, *Water Resour. Res.*, 34(5), 1027-1033, 1998.
- 7 Hollenbeck, K. J., C. F. Harvey, R. Haggerty, and C. J. Werth, A method for estimating
- 8 distributions of mass transfer rate coefficients with application to purging and batch
- 9 experiments, *J. Contam. Hydrol.*, 37(3-4), 367-388, 1999.
- 10 Jaekel, U., A. Georgescu, and H. Vereecken, Asymptotic analysis of nonlinear
- 11 equilibrium solute transport in porous media, *Water Resour. Res.*, 32(10), 3093-
- 12 3098, 1996.
- 13 Kauffman, S. J., C. H. Bolster, G. M. Hornberger, J. S. Herman, and A. L. Mills, Rate-
- 14 limited transport of hydroxyatrazine in an unsaturated soil, *Environ. Sci. Technol.*,
- 15 32(20), 3137-3141, 1998.
- 16 Lafolie, F., and Ch. Hayot, One-dimensional solute transport modelling in aggregated
- 17 porous media, Part 1, Model description and numerical solution, *J. Hydrol.*, 143(1-
- 18 2), 63-83, 1993.
- 19 LePage, W. R., *Complex Variables and the Laplace Transform for Engineers*, McGraw-
- 20 Hill, New York, 1961.
- 21 Lessoff, S. C., and L. F. Konikow, Ambiguity in measuring matrix diffusion with single-
- 22 well injection/recovery tracer tests, *Ground Water*, 35(1), 166-176, 1997

- 1 Lorden, S. W., W. Chen, and L. W. Lion, Experiments and modeling of the transport of
- 2 trichloroethene vapor in unsaturated aquifer material, *Environ. Sci. Technol.*, 32(13),
- 3 2009-2017, 1998.
- 4 McLaren, R. G., C. A. Backes, A. W. Rate, and R. S. Swift, Cadmium and cobalt
- 5 desorption-kinetics from soil clays: Effect of sorption period, *Soil Sci. Soc. Am. J.*,
- 6 62(2), 332-337, 1998.
- 7 Meigs, L. C., and R. L. Beauheim, Tracer tests in a fractured dolomite. 1. Experimental
- 8 design and observed tracer recoveries, submitted to *Water Resour. Res.*, December,
- 9 1998, accepted pending revisions to be completed.
- 10 Meigs, L. C., T. L. Jones, and R. L. Beauheim, editors, Interpretations of Tracer Tests
- 11 Performed in the Culebra Dolomite at the Waste Isolation Pilot Plant Site, *SAND97-*
- 12 *3109*, Sandia National Laboratories, Albuquerque, NM, in press.
- 13 Neretnieks, I., and A. Rasmuson, An approach to modelling radionuclide migration in a
- 14 medium with strongly varying velocity and block sizes along the flow path, *Water*
- 15 *Resour. Res.*, 20(12), 1823-1836, 1984.
- 16 Pedit, J. A., and C. T. Miller, Heterogeneous sorption processes in subsurface systems,
- 17 1., Model formulations and applications, *Environ. Sci. Technol.*, 28(12), 2094-2104,
- 18 1994.
- 19 Pedit, J. A., and C. T. Miller, Heterogeneous sorption processes in subsurface systems. 2.
- 20 Diffusion modeling approaches, *Environ. Sci. Technol.*, 29(7), 1766-1772, 1995.
- 21 Peszynska, M., Finite element approximation of diffusion equations with convolution
- 22 terms, *Math. Comp.*, 65(215), 1019-1037, 1996.

1 Rao, P. S. C., D. E. Rolston, R. E. Jessup, and J. M. Davidson, Solute transport in
2 aggregated porous media: Theoretical and experimental evaluation, *Soil Sci. Soc. Am. J.*, 44(6), 1139-1146, 1980.

4 Rao, P. S. C., R. E. Jessup, and T. M. Addiscott, Experimental and theoretical aspects of
5 solute diffusion in spherical and nonspherical aggregates, *Soil Sci.*, 133(6), 342-349,
6 1982.

7 Rasmussen, A., The effect of particles of variable size, shape and properties on the
8 dynamics of fixed beds, *Chem. Eng. Sci.*, 40(4), 621-629, 1985.

9 Roberts, G. E., and H. Kaufman, *Table of Laplace Transforms*, W. B. Saunders Co.,
10 Philadelphia, PA, 1966.

11 Ruthven, D. M., and K. F. Loughlin, The effect of crystallite shape and size distribution
12 on diffusion measurements in molecular sieves, *Chem. Eng. Sci.*, 26(5), 577-584,
13 1971.

14 Sahoo, D., and J. A. Smith, Enhanced trichloroethene desorption from long-term
15 contaminated soil using triton X-100 and pH increases, *Environ. Sci. Technol.*,
16 31(7), 1910-1915, 1997.

17 Scher, H., M. F. Shlesinger, and J. T. Bendler, Time-scale invariance in transport and
18 relaxation, *Phys. Today*, 44(1), 26-34, 1991.

19 Stager, M. P., and G. P. Perram, Long-term desorption of trichloroethylene from flint
20 clay using multiplexed optical detection, *Environ. Poll.*, 104(3), 397-400, 1999.

21 Valocchi, A. J., Use of temporal moment analysis to study reactive solute transport in
22 aggregated porous media, *Geoderma*, 46(1/3), 233-247, 1990.

1 van Genuchten, M. Th., and P. J. Wierenga, Mass transfer studies in sorbing porous
2 media. 1. Analytical solutions, *Soil Sci. Soc. Am. J.*, 40(4), 473-480, 1976.

3 Vereecken, H., U. Jaekel, and A. Georgescu, Asymptotic analysis of solute transport with
4 linear nonequilibrium sorption in porous media, *Transp. Porous Media*, 36(2), 189-
5 210, 1999.

6 Villermaux, J., Deformation of chromatographic peaks under the influence of mass
7 transfer phenomena, *J. Chromatographic Sci.*, 12, 822-831, 1974.

8 Villermaux, J., Theory of linear chromatography, in *Percolation Processes: Theory and*
9 *Applications*, edited by E. Rodrigues and D. Tondeur, NATO ASI Series E, vol. 33,
10 Sijthoff and Noordhoff, Rockville, MD, 83-140, 1981.

11 Wagner, B. J., and J. W. Harvey, Experimental design for estimating parameters of rate-
12 limited mass transfer: Analysis of stream tracer studies, *Water Resour. Res.*, 33(7),
13 1731-1741, 1997.

14 Werth, C. J., J. A. Cunningham, P. V. Roberts, and M. Reinhard, Effects of grain-scale
15 mass transfer on the transport of volatile organics through sediments. 2. Column
16 results, *Water Resour. Res.*, 33(12), 2727-2740, 1997.

17 Acknowledgments

18 This work was funded by Sandia National Laboratories and by the Swedish Nuclear Fuel
19 and Waste Management Co. (SKB). Sandia is a multiprogram laboratory operated by
20 Sandia Corporation, a Lockheed Martin Company, for the United States Department of
21 Energy under Contract DE-AC04-94AL85000. R.H. would like to thank A.T. Zoes for

1 helpful conversations in regard to this work. We are grateful for reviews by V.
2 Cvetkovic, B. Davis, S. Geiger, and P. Reeves, and for logistical support provided by M.
3 Kelley.

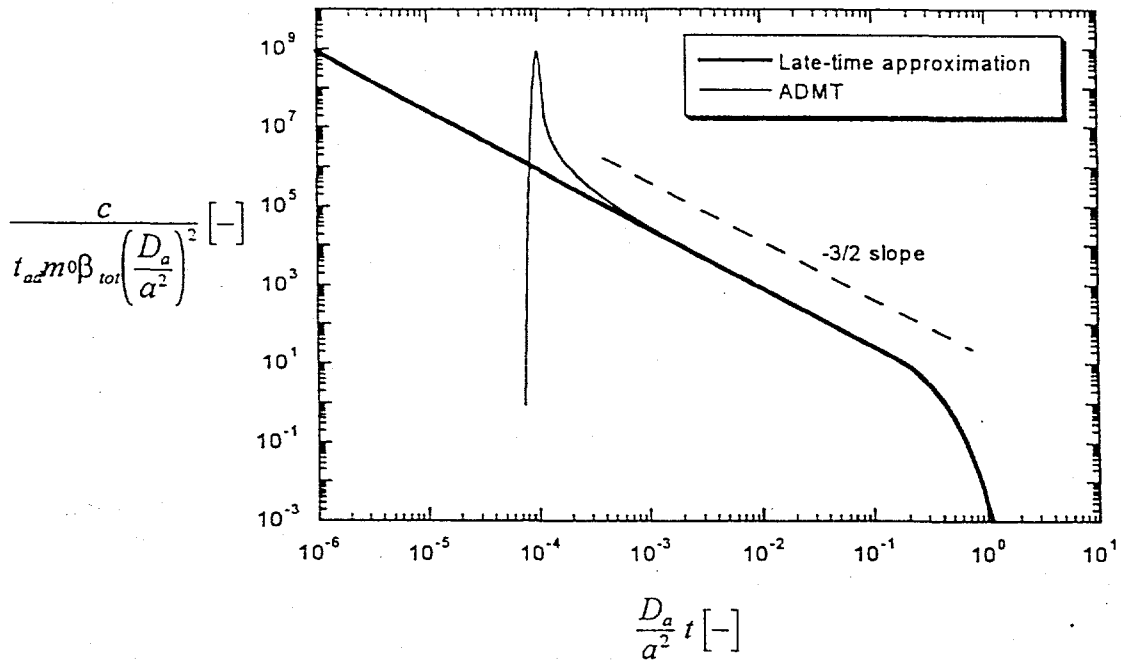


Figure 1: Late-time solution and full ADMT solution for spherical diffusion.

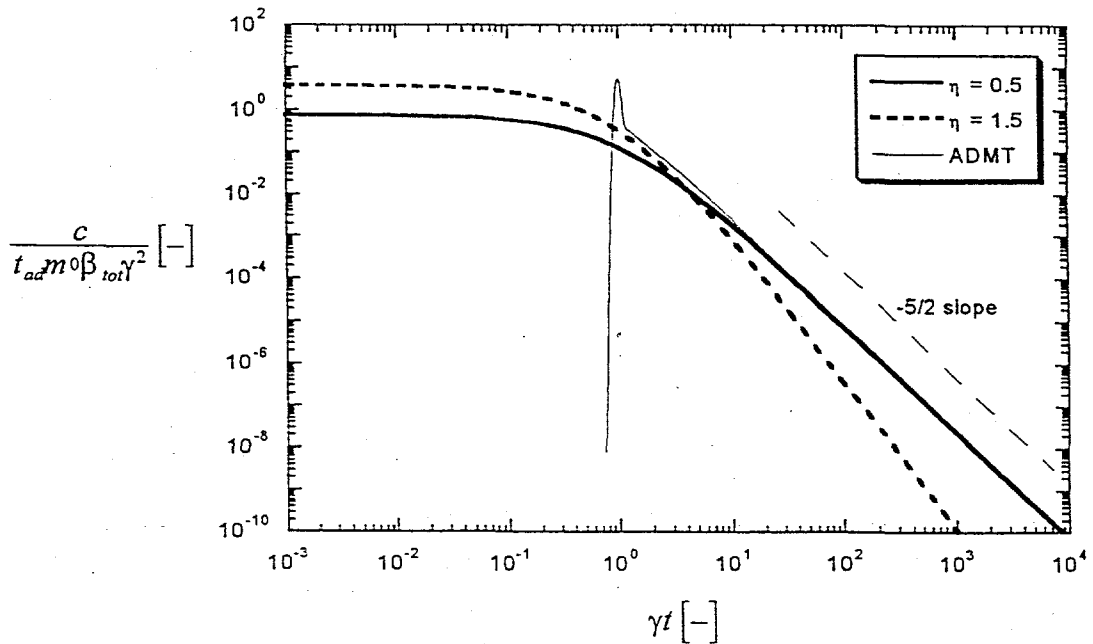


Figure 2: Late-time solution and full ADMT solution for gamma distribution of first-order rate coefficients.

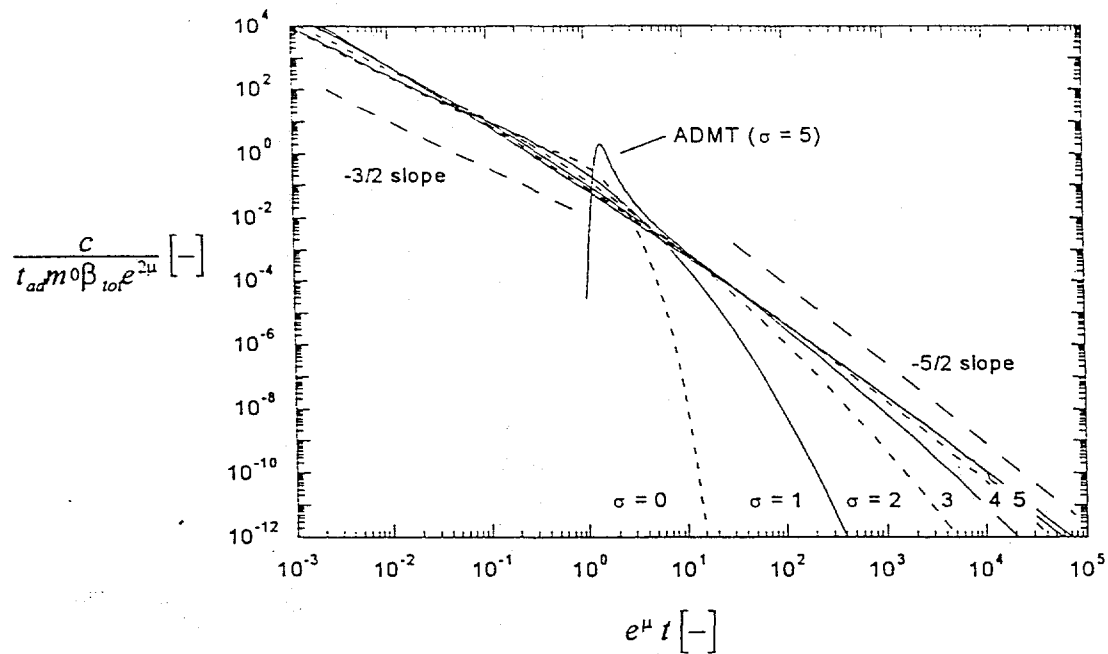


Figure 3: Late-time solution and full ADMT solution for lognormal distribution of diffusion rate coefficients. The value e^μ is the geometric mean of the distribution.

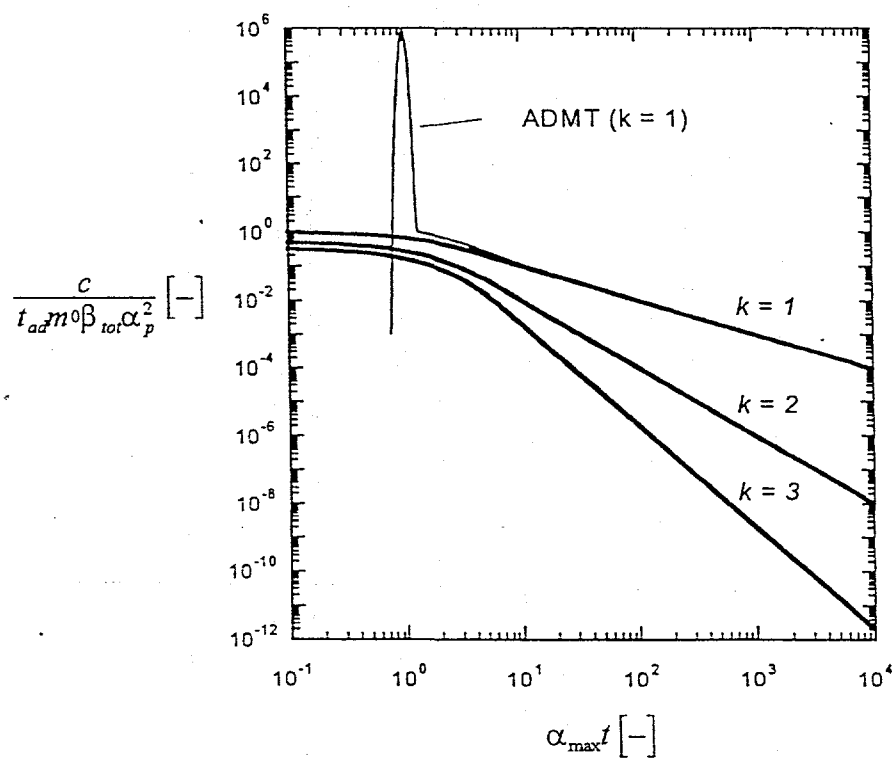


Figure 4: Late-time solution and full ADMT solution for power-law distribution of first-order rate coefficients.

Figure
will be
revised
so line width
increases
as σ increases

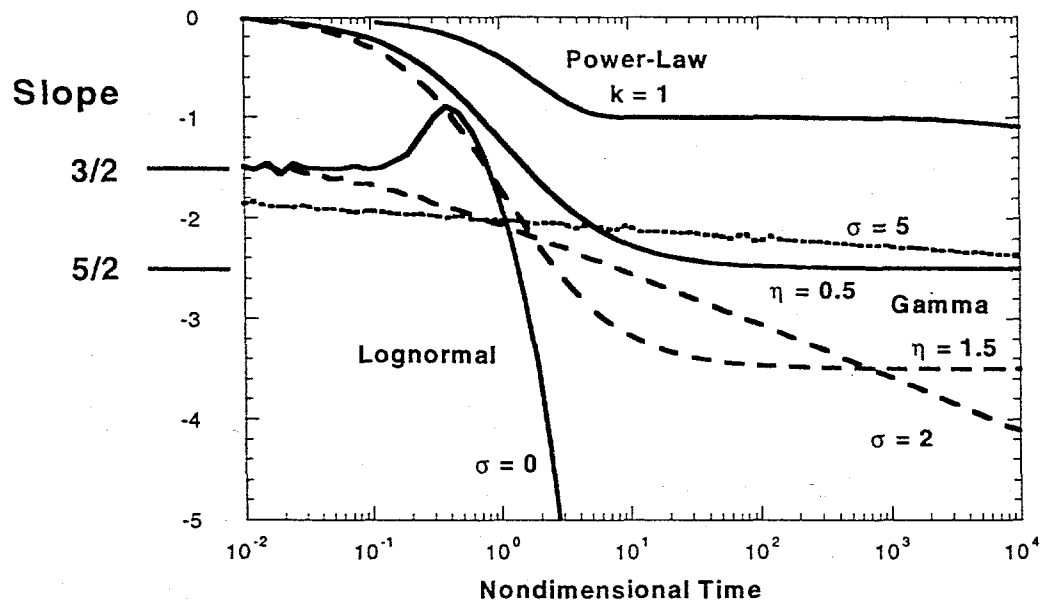


Figure 5: Slopes of late-time double-log breakthrough curves. Note that during the time that the BTC is dominated by advection and dispersion (i.e., at early time), the slopes will be different from those shown here. Nondimensional time is given as in Figures 2, 3, and 4 for each of the models.

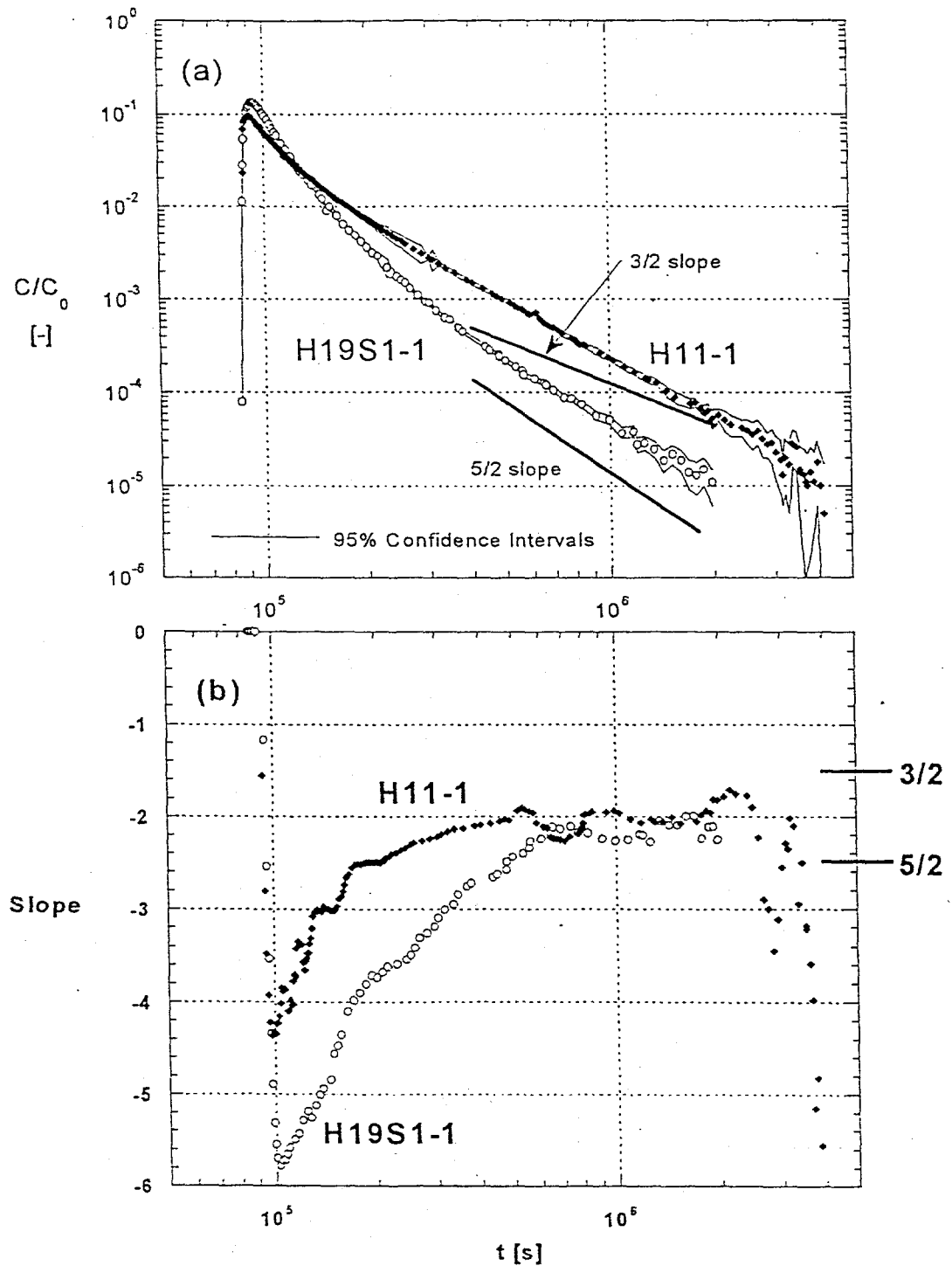


Figure 6: Plots of SWIW data from the WIPP site (a) and the slopes of the data (b). For comparison of slopes to conventional diffusion, the extra lines in 6(a) have slopes of $3/2$ and $5/2$. Confidence intervals (95%) are shown as thin solid lines above and below the data.